available at www.sciencedirect.com

ScienceDirect

journal homepage: www.elsevier.com/locate/agrformet

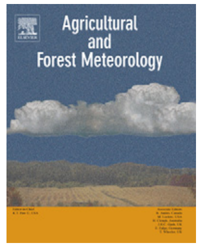

Effects of different eddy covariance correction schemes on energy balance closure and comparisons with the modified Bowen ratio system

Adam Wolf[a,*], *Nick Saliendra*[b], *Kanat Akshalov*[c], *Douglas A. Johnson*[d], *Emilio Laca*[e]

[a] *Carnegie Institution of Washington, Department of Global Ecology, 260 Panama Street, Stanford, CA 94305, USA*
[b] *USDA Forest Service, Forestry Sciences Laboratory, Rhinelander, WI 54501, USA*
[c] *Baraev Kazakh Research Institute for Grain Farming, Akmolinskaya Oblast, Shortandy 474010, Kazakhstan*
[d] *USDA-ARS Forest and Range Research Lab, Utah State University, Logan, UT 84322-6300, USA*
[e] *Department of Plant Sciences, University of California, Davis, CA 95616, USA*

ARTICLE INFO

Article history:
Received 4 October 2007
Received in revised form
8 January 2008
Accepted 9 January 2008

Keywords:
Eddy covariance
Modified Bowen ratio
Flux correction

ABSTRACT

Eddy covariance (EC) and modified Bowen ratio (MBR) systems have been shown to yield subtly different estimates of sensible heat (*H*), latent heat (LE), and CO_2 fluxes (Fc). Our study analyzed the discrepancies between these two systems by first considering the role of the data processing algorithm used to estimate fluxes using EC and later examining the effects of atmospheric stability on discrepancies between EC and MBR. We found that EC correction algorithms disproportionately increase the magnitude of LE and Fc, and consequently have a strong effect on the Bowen ratio measured by EC. Two corrections not universally employed were each found to account for up to 20% of LE and Fc: the correction for signal asynchrony by adjusting the lag between the IRGA and the sonic anemometer, and the frequency domain correction for path-length averaging in both instruments. Comparison of fluxes between two EC systems 10 m apart showed that LE and Fc are inherently more variable than *H*, highlighting the role of field heterogeneity in determining canopy gas exchange at very small spatial scales.

When all relevant corrections were applied, there was no bias for *H* and LE between EC and MBR. An examination of discrepancies between EC and MBR showed that the discrepancies were highest during neutral periods when shear drove vertical mixing much more than buoyancy. During these neutral periods, the correlation between T, H_2O, and CO_2 was much lower on average, which violates the similarity assumption exploited in the MBR technique. The largest discrepancies in Fc in both systems were clearly visible when plotted against a light–response curve, which creates the possibility of using a screening technique to exclude data that depart markedly from other recently collected data. The EC system tended to have the largest departures from the expected value at low light and during the night, while the MBR system tended to show occasionally spikes of high photosynthetic uptake.

* *Corresponding author.*
E-mail address: adamwolf@stanford.edu (A. Wolf).
0168-1923/$ – see front matter
doi:10.1016/j.agrformet.2008.01.005

1. Introduction

Bowen ratio-energy balance (BREB) is a widely used technique for measuring surface water and heat exchange (e.g., Gao et al., 1998; Hope and Evans, 1992), and owes much of its success to its ease of use, simple theoretical basis, and relatively modest instrumental requirements. The term "modified Bowen ratio" (MBR) has been adopted for systems which use the BREB technique to measure additional traces gases, in particular CO_2 (Hall and Claiborn, 1997; Lindberg et al., 1995; Meyers et al., 1996; Muller et al., 1993; Schween et al., 1997). Eddy covariance (EC) is a more recent technique that has several distinct advantages, particularly for observations over tall canopies (Baldocchi et al., 2001), but takes considerably more effort to maintain, process, and quality assure results for long-term measurements (Aubinet et al., 2000; Papale et al., 2006). Considerable interest exists in using these systems to measure net ecosystem CO_2 and H_2O exchange across long time periods where integrals of measurement errors can become large (Moncrieff et al., 1996). As a result, there is a compelling need to ensure that the inferences of the magnitude of the source/sink strength in different ecosystems does not depend on the way CO_2 and H_2O fluxes are measured (Brotzge and Crawford, 2003; Liu and Foken, 2001). Agreement of EC and MBR measurements during the daytime rests on two factors. The foremost factor is the accuracy of measuring energy fluxes into the surface, including net radiation (Rn), ground heat flux (*G*), and ground storage (*S*), which directly determine the magnitude of $H + LE$ for the BR system, and which constitutes a measure of energy balance closure in EC studies. A second factor is the different bias of the two systems in partitioning available energy toward either *H* or LE.

Although Massman and Lee (2002) discussed many EC data processing issues, few intercomparisons have focused on the role of data processing schemes as a source of measurement differences among research groups, or between direct comparisons between EC and MBR. Networks of flux towers require intercomparability among systems (Baldocchi et al., 2001), which is difficult to attain when both the instrumentation and correction schemes vary (Loescher et al., 2006). While standardization in data processing remains a goal for research using eddy covariance stations, considerable variation exists in data collection and archiving procedures, preprocessing of high frequency data, and postprocessing of covariance data (Twine et al., 2000).

This paper does not focus on the theory of the corrections themselves, but instead examines the consequences of different correction procedures on a dataset of CO_2 and energy fluxes above a grassland. We hypothesize that a major cause of lack of energy balance closure and incomparability between EC and MBR is the correction algorithm used to process EC data.

2. Methods

Some of the major facets of EC correction are briefly outlined below for reference.

Coordinate rotation: Covariances should be rotated to a natural coordinate system (Lee et al., 2004) to partially fulfill a key assumption of the EC technique, namely that the flux measurement represents the flux perpendicular to the surface out of a nominal control volume defined at its top by the sensor and neglecting horizontal divergence so that the system becomes one-dimensional (Moncrieff et al., 2004). The classical coordinate rotation is straightforward to compute with a full suite of three-dimensional gas and wind covariances for each measurement period and is widely applied albeit not universally (Twine et al., 2000).

Air density correction: Density variations introduced by fluctuations of temperature and moisture content of air in updrafts and downdrafts create spurious fluxes when air is measured volumetrically. The correction of H_2O and CO_2 fluxes due to effects of temperature and H_2O on air density and non-zero mean vertical wind speed has long been a standard correction to EC measurements (Webb et al., 1980).

Frequency-dependent signal loss: Moore (1986) and Massman (2000) outlined a number of factors that affect the frequency response of the measured scalars and winds, including averaging over the sensor path, asynchrony between the measured signals (by spatial separation or by delays introduced by the instrumentation itself), analog filtering of the measurements before they are recorded, and detrending of the raw time series. Use of an inappropriate averaging interval also introduces loss of low-frequency components of the flux (Foken et al., 2006). All of these frequency-dependent effects result in a loss of signal variance, and hence decrease the flux estimated by eddy covariance. The signal asynchrony between two signals can be addressed by finding the lag between them at which their absolute correlation is maximized for a given measurement period, and applying flux calculations using this lag (Eugster et al., 1997). Path-length averaging and de-trending require calculation of a transfer function in the frequency domain for unfiltering the data (Rissmann and Tetzlaff, 1994), or using an assumed shape of the cospectrum and estimating stability-dependent correction factors based on empirical filter coefficients (Massman, 2000). An experiment described in a companion paper shows that signal loss is also possible if the measurements are taken at too low a frequency, a problem which is most evident during neutral (high shear) conditions and low observation height (Wolf and Laca, in press).

2.1. *Study setup and location*

Measurements were taken in five intervals of several days each from May to September 2001. Data were collected continuously by MBR, but the EC system was transported to several sites in the region, so the instruments were only co-located for 22 total days. In addition, a second EC system was located at the site for 5 days, allowing a direct estimate of the EC measurement error. All of the systems were located within 20 m of each other. The data represent a wide range of meteorological conditions during the season, including day, night, wet, dry, growing, and senescent periods. The study site was located in the shortgrass steppe region of Kazakhstan, 40 km north of the capital Astana, on the experimental station of the Baraev Kazakh Research Institute for Grain Crops

Research. The site was a 200 ha pristine grass-forb steppe at 51.5758 N, 71.2681 E, 428 m above sea level. The fetches for upwind directions were 250 m from the north, 610 m from the east, 2250 m from south, and 360 m from the west, beyond which were fallow wheat fields. The site is extraordinarily flat with no slopes exceeding 0.5° for 20 km in any direction, and only isolated trees with none nearer than 5 km to the towers. The canopy height of the vegetation was about 0.3 m. A description of the ecology and meteorology of the site is available in Wolf et al. (2006).

2.2. EC measurement

EC measurements of CO_2, H_2O, and heat fluxes are based on a fast-response open-path infrared gas analyzer (IRGA; model LI-7500, Licor, Inc., Lincoln, NE) coupled with a three-dimensional sonic anemometer (model CSAT-3, Campbell Scientific Inc., Logan, UT, henceforth CSI), both installed at 1.3 m above ground level. Digital signals from these instruments were recorded at 10 Hz using a Campbell Scientific CR5000 datalogger. Raw data were archived for later processing.

2.3. EC data processing

Data were processed in several steps to compute fluxes. The steps in flux processing were: parsing data into 20 min intervals; recursively removing spikes greater than 6σ beyond a quadratic fit to the 10 Hz data; dealiasing with a first order Butterworth filter with a cutoff frequency at 4.8 Hz (Fisher, 2007), which had the recurrence relation:

$$y_t = 0.94165478x_t + 0.94165478x_{t-1} - 0.8833089876y_{t-1} \quad (1)$$

where x is the original scalar time series and y is the filtered time series; rotation to a natural coordinate system (Lee et al., 2004); removing signal asynchrony by maximizing the covariance between each scalar and the vertical wind (e.g., Eugster et al. (1997)); calculating scalar fluxes using the mean and covariance of each scalar with the vertical wind, making frequency domain corrections to the fluxes for path-length averaging using the filter coefficients summarized in Massman (2000); and adjusting fluxes for air density artifacts (Webb et al., 1980). The antialiasing filter does not affect the results of this study, but was applied to allow comparison with a cospectral analysis of these data presented elsewhere (Wolf and Laca, in press).

Coordinate rotation (CR), signal asynchrony correction (LAG), density correction (WPL), and Massman's (2000) frequency-response correction (FR) were examined alone and in combination for their effects on the sensible heat (H), latent heat (LE), and CO_2 fluxes (Fc) calculated from EC measurements.

2.4. MBR measurement

We used the Bowen ratio-energy balance (BREB; model 023/CO_2 Bowen Ratio, CSI) system for continuous measurements of energy, water vapor, and CO_2 fluxes at the study site. The theory and operation of the BREB technique were described in detail by Dugas et al. (1999). Water vapor and CO_2 concentrations were measured with an infrared gas analyzer (IRGA; model LI-6262, Li-Cor Inc., Lincoln, NE, USA) in differential mode with the CO_2 and water vapor scrubbed on the chopper input. Air samples from two heights (0.7 and 1.7 m above the soil surface) were drawn and routed to the IRGA, which measured the difference in water vapor and CO_2 concentrations between the two heights. Average canopy height of the vegetation at peak growth was about 0.5 m, thus the two air sampling heights were about 0.2 and 1.2 above the vegetation's surface. A low-power pump (model TD-3LSC; Brailsford & Co., Inc., Rye, NY, USA) aspirated the air through 1-μm teflon filters (model Acro 50; Gelman Sciences, Ann Arbor, MI, USA), which prevented dust and liquid water contamination in the air tubes and IRGA. A solenoid valve (model 236-102B, Numatics Inc., Highland, MI, USA) was programmed to reverse the air drawn through the IRGA sample and reference cells every 2 min. Another solenoid valve was programmed to control the air stream at the beginning of each hour, when the IRGA sample cell was scrubbed to determine absolute concentrations of CO_2 and water vapor. The difference of air temperature between the two heights was measured with fine-wire chromel-constantan thermocouples (model FW3, CSI). The differences of temperature and concentrations of water vapor and CO_2 between the two heights were simultaneously measured every second, and the mean of the differences were calculated and stored every 20 min with a data logger (model CR23X, CSI).

Available energy was measured as the sum of net radiation (Rn, W m^{-2}), ground heat flux (G, W m^{-2}), and soil heat storage (S, W m^{-2}). Rn was measured using two model Q*7.1 net radiometers (REBS, Seattle, WA, USA). G was measured using six sets of soil heat flux plates (two model HFT3, REBS; and four model HFP01SC, Hukseflux thermal sensors, The Netherlands) placed 8 cm below the soil surface. Soil heat storage was estimated using 12 averaging soil temperature probes (model TCAV, CSI) installed in pairs at 2 and 6 cm above the heat flux plates. Heat capacity of the soil was estimated using volumetric soil water content (VSMC) at a 0.05 m depth using a soil moisture content reflectometer (model CS615; CSI) and measured soil bulk density. Physical properties of air were determined with a temperature (Tair) and relative humidity (RH) probe (HMP45C, Vaisala, Finland). Photosynthetically active radiation (PAR) was measured with the LiCor Model LI-190SA quantum sensor. Wind speed (U) and direction were measured using the R.M. Young wind sentry cup anemometer and vane.

2.5. MBR data processing

The Bowen ratio (β) was calculated using vertical gradients of temperature (ΔT, °K) and water vapor (Δq, mmol mol^{-1}) at 20-min averaging intervals:

$$\beta = \left(\frac{C_p}{\lambda 0.622}\right)\left(\frac{\Delta T}{\Delta q}\right) \quad (2)$$

where C_p is the specific heat at constant pressure (1.00467 J g^{-1} K^{-1}), λ is the latent heat of vaporization (J g^{-1}; λ = 3149–2.370·T(°K)), 0.622 is the ratio of molecular weights of water and air. H (W m^{-2}) was calculated as $H = (\mathrm{Rn} - G)/(1 + \beta^{-1})$, and LE (W m^{-2}) was calculated as the residual energy; LE = Rn $-H - G$. The eddy diffusivity for heat (K_h, m^2 s^{-1}) was calculated as:

$$K_h = \left(\frac{H}{\rho C_p}\right) \cdot \left(\frac{\Delta z}{\Delta T}\right) \tag{3}$$

where ρ is air density (g m^{-3}) and Δz is the height difference (1 m) between the upper and lower thermocouples. Assuming that the eddy diffusivity for CO_2 (K_c) was equal to K_h, the net ecosystem CO_2 flux (μmol m^{-2} s^{-1}) was calculated as:

$$F_{CO_2} = K_c \cdot \left(\frac{\Delta C}{\Delta z}\right) \cdot \left(\frac{100}{44}\right) \tag{4}$$

where ΔC is the difference in CO_2 density (mg m^{-3}) between the two heights and (1000/44) is a factor to convert Fc from mg m^{-2} s^{-1} to μmol m^{-2} s^{-1}. Fc was corrected for the difference in water vapor density between the two heights (Webb et al., 1980), but not for heat density effects, because fine-wire thermocouple measurements of the two air streams immediately upstream of the IRGA have been shown to be nearly identical in many towers with the same instrumental setup in US rangelands (Angell et al., 2001).

3. Results

3.1. *Instrument comparison*

Comparisons between sensors are summarized in Table 1. There was overall close agreement between the net radiometers, although at the highest light levels a discrepancy of up to 50 W m^{-2} was observed. Other meteorological measurements (PAR, T, RH, U) were likewise very consistent. The poorest agreement was found among the soil measurements (Tsoil, G, and VSMC). Note that the G measurements using the two sets of REBS plates were permanently installed to accompany the MBR system, whereas the Hukseflux plates were removed and reinstalled each time the EC system was moved. The permanently installed REBS plates and Tsoil sensors made very similar estimates of G and S, but the Hukseflux plates that were moved and reinstalled varied more widely, and had different amplitudes, apparently due to subtle differences in their vertical placement in the soil or the conductivity of the soil. Therefore, while the contribution of G and S terms to the overall energy budget is small compared to Rn, the difference between individual measurements of G and S can be quite large relative to the mean G or S. By contrast, different estimates of Rn tend to be very similar, but because Rn is a large term in the energy budget, the differences between observations can be occasionally large. Because of these differences in the relative contributions of Rn, G and S to the energy budget, and the relative uncertainty in their measurement, they had similar contributions (up to 50 W m^2) to the absolute uncertainty in available energy (AE = Rn + G + S).

Table 1 – Comparisons between instrument arrays with the first row from the EC system and the second row from the MBR system, with the exception of the intercomparison between the REBS heat flux plates

Instrument 1	Tair HMP45	RH HMP45	ea HMP45	H_2O Li7500	CO_2 Li7500	U dir CSAT	U CSAT	Rain gage	Rn	PAR	G Hukse average	G REBS	Tsoil	VSMC	S
Instrument 2	Tair HMP45	RH HMP45	ea HMP45	H_2O HMP45	CO_2 Li6200	U dir vane	U cup	Rain gage	Rn	PAR	G REBS average	G REBS	Tsoil	VSMC	S
R^2	0.99	0.99	0.99	0.93	0.31	0.93	0.93	0.95	0.99	0.99	0.84	0.96	0.91	0.82	0.87
Slope	0.99	0.98	0.99	0.82	0.44	0.99	1.17	0.88	0.96	0.98	0.80	0.69	1.16	0.57	1.42
Intercept	0.06	0.08	−0.01	1.39	197	6.12	−0.01	0.00	−0.13	2.71	2.78	0.83	−1.90	0.05	−0.22
RMSE	0.22	2.49	0.02	0.45	11.01	27.03	0.63	0.04	8.23	46.68	7.87	3.01	1.37	0.02	14.2
N	2287	2287	2287	2105	2123	2142	2160	2287	2280	2326	2326	2326	2287	2218	2326

The slope and intercept are for the regression equation Instrument 2 = slope × Instrument 1 + intercept.

Table 2 – Comparisons between data that were partially corrected and fully corrected. Corrections included signal asynchrony (LAG), coordinate rotation (CR), buoyancy correction (WPL), and path-length averaging (FR)

Flux term	EC corrections applied											
	WPL		CR–WPL		CR–WPL–FR		LAG–WPL		LAG–CR–WPL		LAG–CR–WPL–FR	
	Slope	R^2	Slope	R^2	Slope	R^2	Slope	R^2	Slope	R^2	Slope	R^2
Regression statistics vs. LAG–CR–WPL–FR												
H	0.96	0.97	0.98	0.99	1	1	0.96	0.98	0.98	0.99	1	1
LE	0.73	0.96	0.76	0.96	0.92	0.97	0.81	0.97	0.82	0.99	1	1
Fc	0.60	0.72	0.60	0.80	0.76	0.83	0.80	0.90	0.81	0.99	1	1
H + LE	0.85	0.98	0.87	0.98	0.96	0.99	0.89	0.98	0.90	0.99	1	1
Bowen ratio	1.23		1.33		1.03		1.18		1.27			
(Bowen ratio)^2	0.032	0.84	0.045	0.94	0.00	0.96	0.03	0.87	0.044	0.98	1	1

The slopes represent the slope coefficient of the correction suite in each column regressed on the fully corrected data.

3.2. *Effect of correction procedures and EC/MBR comparison*

Different correction schemes to process the EC data resulted in major differences in flux estimates, in particular for LE and Fc, and by extension the Bowen ratio (Table 2). For example, Fc that was only WPL corrected was only 60% as large as Fc that was corrected by LAG, CR, WPL, and FR. The largest contribution comes from the LAG correction, which increases Fc about 24% (although this correction increased LE by a more modest 8%) in the full correction. The FR correction also had a major impact on the fluxes, and increased LE and Fc by 15–18%. The heat flux was only affected by 2% on average by CR or FR corrections.

Energy balance closure for EC was analyzed by the slope of the regression between outgoing turbulent energy (TE = H + LE) against different metrics of AE (Table 3). Different estimates of TE were obtained by using different correction schemes as outlined above. Three different estimates of AE were used. The mean AE sums the mean of each energy balance term measured by the different instruments. The maximum and minimum AE sums the individual instruments that measured the maximum or minimum values of Rn, G and S, thus giving a range of estimates of these energy balance components. Using mean AE, the energy balance was strongly influenced by the correction regime, and increased more than 10% from using only WPL to using LAG, CR, WPL, and FR together. An additional 5% of energy balance was lost or gained when using the minimum or maximum AE, indicating that instrumental variation and data processing were comparatively large influences on the inferred energy balance.

Comparisons of H, LE and Fc between the two EC systems (processed using all corrections described above) are presented in Table 4. H was remarkably consistent between the two systems (R^2 = 0.98), followed by LE (R^2 = 0.93) (Fig. 1a and b). By contrast, distinctly greater scatter was observed in Fc between the two systems (R^2 = 0.88), although the slope was not significantly different from one (Fig. 1c). Statistical analysis of the differences between the two systems in H, LE and Fc show that the errors are not normally distributed, due to a sharp peak at zero and a few large departures. This leptokurtic distribution is characteristic of the difference between two exponentially distributed variables, and is best described using the Laplace (double exponential) distribution (Hollinger and Richardson, 2005). The Laplace distribution estimates the dispersion of data using parameter β (analogous to the standard deviation σ in a Gaussian distribution), which is equal to the mean absolute deviation from the median (μ) of the data. The β parameter for all of the fluxes is about half of σ (Table 4).

Differences between EC and MBR were generally larger than between the two EC systems, but no strong biases were

Table 3 – Energy balance closure estimated using different correction schemes to estimate turbulent energy (H + LE) and different instrument arrays to estimate available energy (AE = Rn + G + S)

Flux terms:	EC corrections applied					
	WPL	CR–WPL	CR–WPL–FR	LAG–WPL	LAG–CR–WPL	LAG–CR–WPL–FR
Slope of (H + LE) vs. (Rn + G + S)						
(H + LE) vs. min. {Rn + G + S}	0.81	0.81	0.90	0.83	0.84	0.93
(H + LE) vs. avg. {Rn + G + S}	0.77	0.77	0.85	0.79	0.79	0.88
(H + LE) vs. max. {Rn + G + S}	0.72	0.73	0.80	0.75	0.75	0.83
Absolute value of (H + LE)–avg. {Rn + G + S} in W m^{-2}						
Mean	32.0	32.5	24.0	27.6	28.1	18.9
Median	19.0	18.9	13.6	16.3	16.2	11.1

The average AE was calculated as a mean of all instruments, whereas the maximum and minimum AE were calculated using the combination of instruments producing the maximum or minimum total AE.

Table 4 – Comparisons between flux measurements

Instrument 1:	H EC	LE EC	Fc EC	H EC	LE EC	Fc EC
Instrument 2:	H EC	LE EC	Fc EC	H MBR	LE MBR	Fc MBR
R^2	0.98	0.93	0.88	0.72	0.71	0.59
Slope	1.00	1.00	0.99	1.05	1.02	0.91
Intercept	1.00	0.94	−0.12	11.63	10.65	−0.16
RMSE	10.47	18.15	1.05	45.34	41.08	2.01
Laplace-β	5.51	9.36	0.45	29.75	25.11	1.57
Median	−0.99	−0.24	0.00	4.58	1.77	0.00
N	313	312	311	699	699	699

The EC measurements have all been processed using the full suite of correction procedures (LAG–CR–WPL–FR) described in the text. Laplace-β is the dispersion parameter of the Laplace distribution.

observed between the two systems (Fig. 2). As in the EC–EC comparison, *H* ($R^2 = 0.72$) and LE ($R^2 = 0.71$) were most similar to each other, and Fc ($R^2 = 0.61$) exhibited more scatter (Table 4). Similar to the EC-EC differences, the EC-MBR differences were leptokurtic and not normally distributed, yielding values for the Laplace dispersion parameter β that were smaller than their respective RMSE statistics, underscoring occasionally large differences between the two sets of observations, but overall differing little.

3.3. *Analysis of flux differences*

The differences between EC and MBR were analyzed in relation to prevailing meteorological conditions, particularly atmospheric stability. Stability was evaluated using the dimensionless parameter *z/L*, which reflects the relative influence of buoyancy and shear in driving vertical mixing. This dimensionless parameter is the ratio between the measurement height (*z*) to the Obukhov length (*L*). Positive *z/L* indicates a stably stratified boundary layer (typical at night), negative *z/L* indicates an unstable boundary layer (typical during the day), and small values of *z/L* are neutral, where mixing is driven mostly by wind shear. The discrepancy between the fluxes was defined both in absolute terms (Flux EC–Flux MBR) and in relative terms (defined as the absolute value of the difference between the fluxes divided by the mean of the fluxes). The relative difference was used in part to enable comparisons with the correlation coefficients of the scalars, which is a metric of the degree to which scalars are transported in the same eddies. For this analysis, the hours

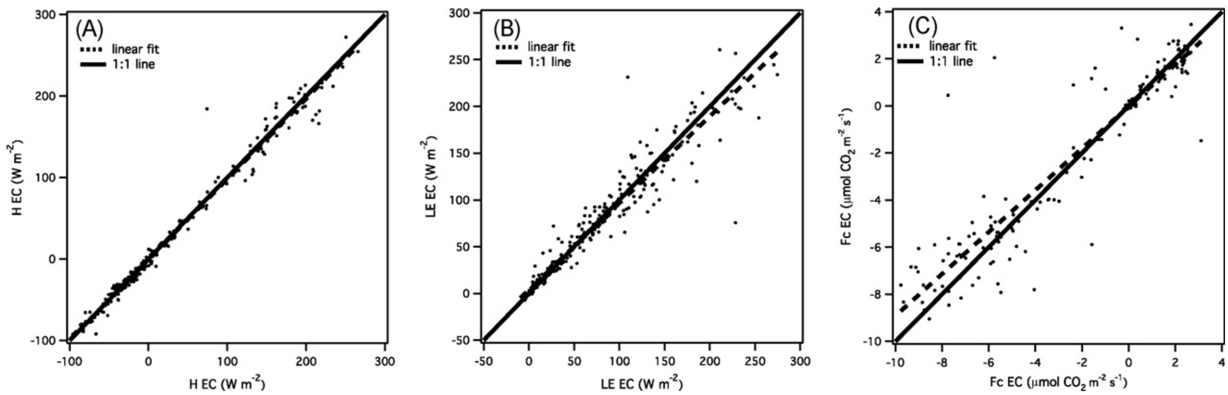

Fig. 1 – Comparisons of *H*, LE and Fc between two EC systems located 10 m apart.

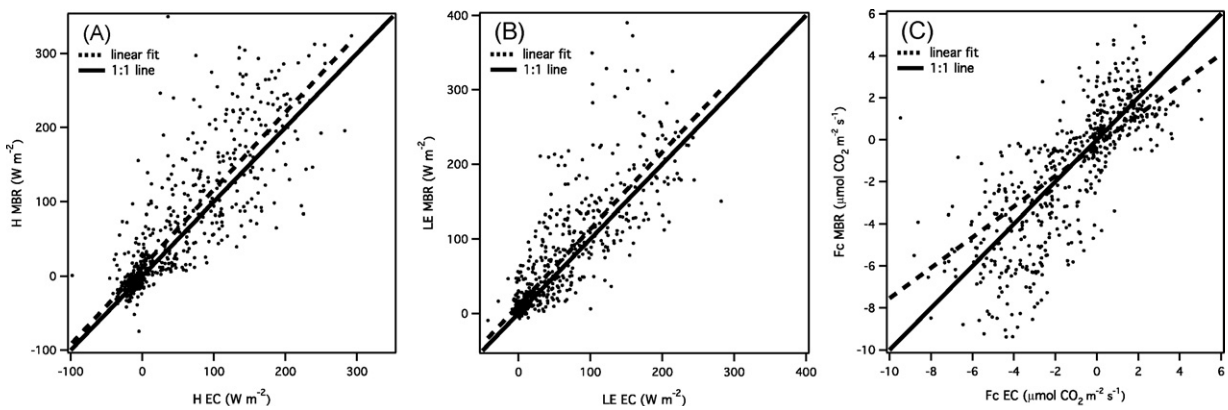

Fig. 2 – Comparisons of *H*, LE, and Fc between an EC and an MBR system located 10 m apart.

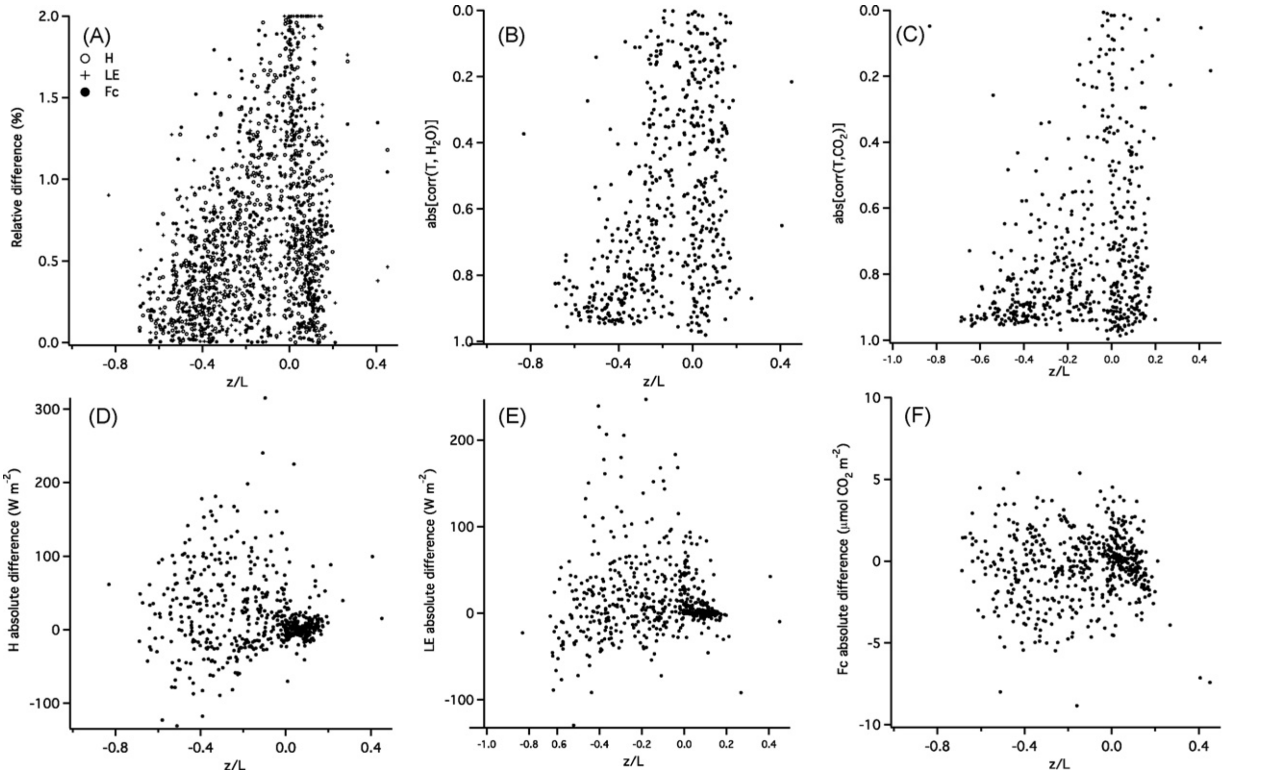

Fig. 3 – Effects of atmospheric stability on the discrepancy between EC-MBR, and on the correlation coefficient between scalars measured by EC. (A) Relative differences of EC and MBR fluxes. (B) Absolute value of correlation coefficient of high frequency T and H_2O measurements. (C) Same as B but for T and CO_2. (D–F) Absolute differences between *H*, LE, and Fc.

preceding and following both sunrise and sunset were removed to avoid periods when fluxes cross or approach zero or when the scalar time series are strongly nonstationary; nonetheless the analysis holds true for these transitional periods as well.

The relative difference was closely linked to stability (Fig. 3a) with a peak at neutrally buoyant conditions for all of the fluxes. However, these were the conditions with the smallest differences in absolute terms (Fig. 3d), a pattern that was also observed for LE (Fig. 3e) but less pronounced for Fc (Fig. 3f). The dependence of the relative difference on stability was clearly reflected by an increased dissimilarity (evaluated as the correlation coefficient between scalars) of turbulent transport of T, H_2O, and CO_2 as stability approached neutral (Fig. 3b and c).

Regardless of the source of the discrepancy, the largest differences in fluxes were clearly discernible as anomalous measurement noise when plotted against a driver such as PAR, or as a time series (Fig. 4).

4. Discussion

The motivation for this study was to determine whether EC and MBR gave similar estimates of surface fluxes for use in parameterizing land surface models for carbon, water, and energy balance studies. Although other studies have addressed this topic previously, none have examined the inherent uncertainty in EC measurements by using two colocated systems, and none have addressed how EC data processing affected parity between the two measurement systems. In addition, the use of two distinct, independent measurement techniques to measure the fluxes allowed us to better interpret possible measurement anomalies.

Data processing had a very strong role in determining the magnitude of EC fluxes. In particular, less commonly applied corrections such as adjusting the lag between the vertical wind speed and the CO_2 and H_2O measurements or correcting for the effects of path-length averaging had larger effect on fluxes than anticipated, each amounting to 20% of the total Fc estimate. The magnitude of these corrections in our study was partly due to the site and tower characteristics, because cospectra of the fluxes at this site peaked at a relatively high dimensionless frequency of 0.1–1, and these corrections act on the high frequency components of the fluxes, with dimensionless frequency greater than 0.1. An extensive discussion of the cospectra of these data and their corrections is given in Wolf and Laca (in press). Judging by the commonly used correction procedures (Twine et al., 2000), few site operators process data using LAG and FR corrections, although as standard software packages begin to be employed, a complete suite of corrections may be more commonly applied.

The magnitude of the EC fluxes has direct implications on the estimated energy balance of the measurements and hence the comparison between EC and MBR, which is forced to close the energy balance. The correction procedures disproportionately increase the LE and Fc fluxes relative to *H*, which clearly affects the Bowen ratio of the EC. Our results showed that as

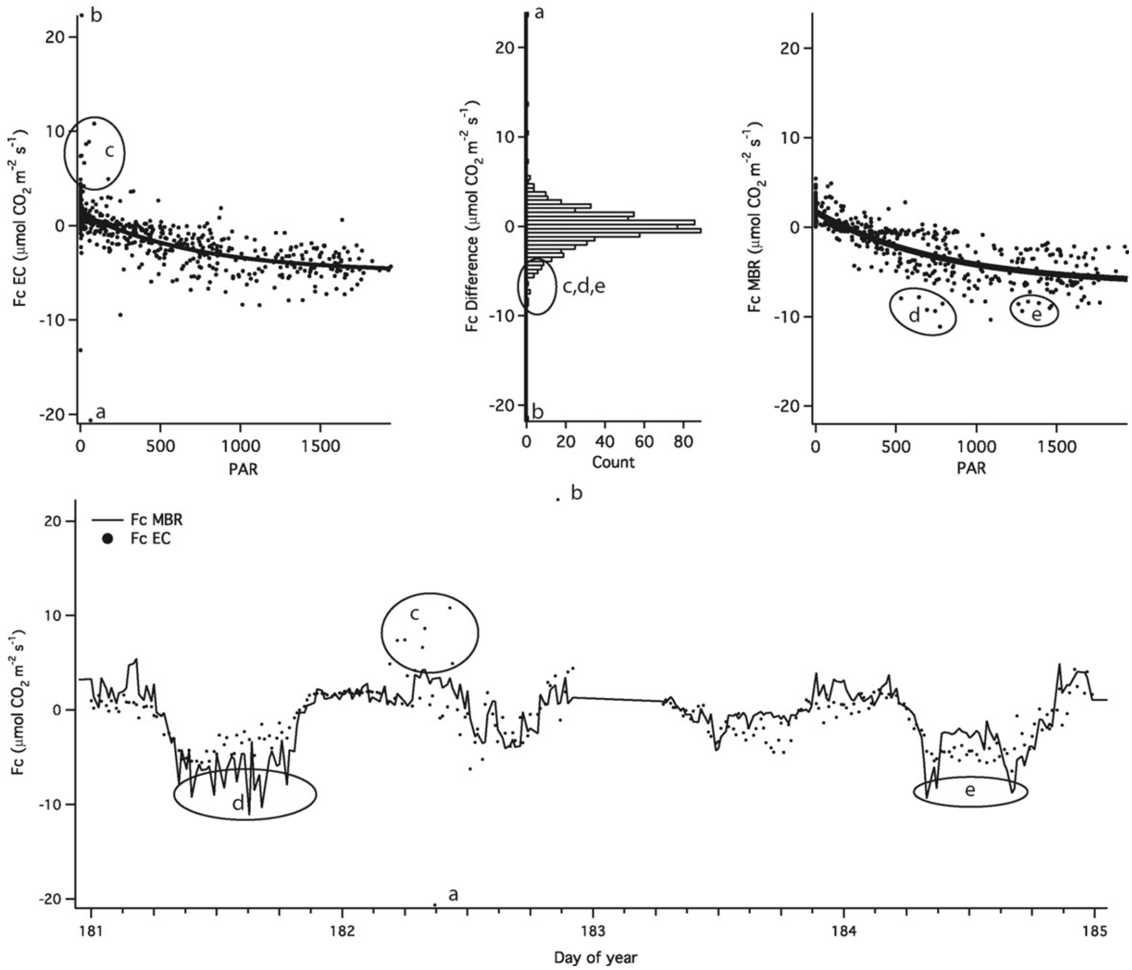

Fig. 4 – Fc measured by EC and MBR plotted against PAR (top right and left), plotted as a representative time series (lower panel; MBR is denoted by a line and EC by dots), and the difference between the two observations (top center). The largest discrepancies between EC and MBR are identified by lower case letters a–e to enhance the comparison of these data between plots.

the EC data were more fully processed, the data more closely approached the magnitude of *H* and LE and hence the Bowen ratio estimated by MBR. This conclusion is supported by the results of previous studies such as Barr et al. (1994), who found that EC tended to have higher Bowen rations (*H*/LE) in comparison to MBR, but who did not use LAG or FR corrections.

It should be pointed out that the choice of averaging period is an additional facet of the EC processing that can have a substantial effect on the observed energy balance (Finnigan et al., 2003; Cava et al., 2007), because short averaging intervals act as a high pass filter that can remove low-frequency components of the turbulent flux under certain circumstances. The potential for loss of flux is particularly high over rough canopies, such as forests, and when measuring at a substantial height relative to the canopy. These measurement conditions lead to a shift in the turbulent cospectrum toward lower frequencies, with consequently greater potential for loss due to short averaging interval. A thorough analysis of the cospectra using the same data from the present study show that the peak of the scalar cospectra for our measurement setup was relatively high-frequency, because the steppe vegetation was relatively smooth and the tower was relatively short (1 m above the canopy). Consequently, the cospectra tapered to zero at the lower frequencies, even with what could be considered a short averaging period (Fig. 5). The loss of flux in the high frequency region of the cospectrum is occasionally high in these data, particularly under neutral stability, but leads to less than 10% loss in energy balance closure under most conditions (Wolf and Laca, in press).

The colocated EC systems in our study measured *H* quite similarly, but showed greater scatter in LE and especially Fc. Canopy physiology has the least influence on *H*, has partial control of the LE due to stomatal regulation of transpiration (but not evaporation from soil), and has total control over Fc, both by photosynthetic uptake and heterotrophic respiration. Apparently, the heterogeneous surface vegetation played a larger than expected role in determining half-hourly surface fluxes in our study.

Hollinger and Richardson's (2005) comparison of paired EC measurements in a forest ecosystem likewise showed that the uncertainty of LE and Fc increased dramatically during the growing season, but the uncertainty of *H* was unaffected by

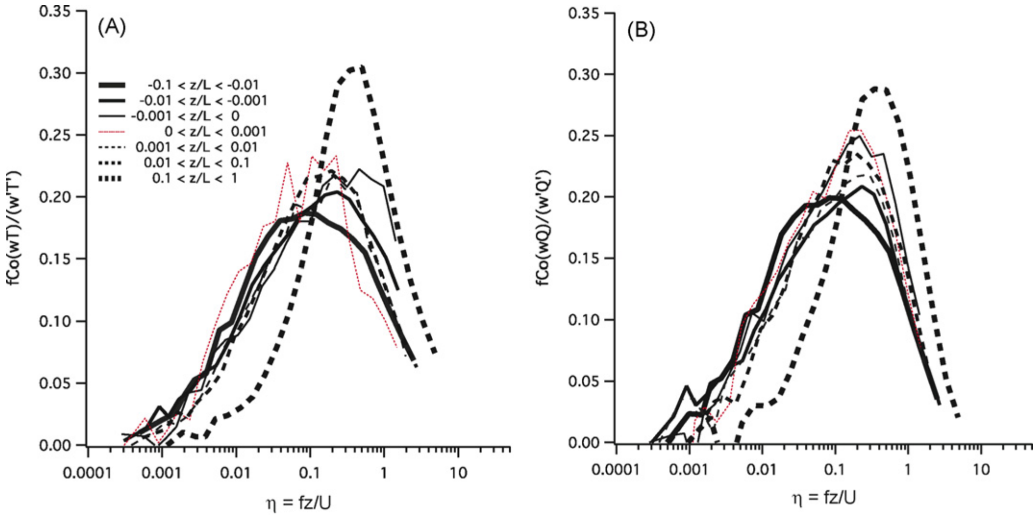

Fig. 5 – Cospectra of sensible heat (A) and latent heat (B), showing dependency of peak shape on stability. The cospectra are ensemble averages for each stability range of all the individual cospectra of the fluxes presented in this study. In all cases, the low frequency components taper to zero.

the phenological state of the vegetation. This suggests that the sources and sinks of heat, water, and CO_2 on the surface are spatially distinct and have different functional controls. *H* is controlled by the thin boundary layer of the elements (leaves, litter, stems, soil) exchanging heat, as well as the temperature gradient between these elements and the atmosphere. LE by contrast is comprised of transpiration, which is controlled by the conductance between the leaf mesophyll and the leaf boundary layer and the corresponding vapor gradient, and of evaporation, which is controlled by the wetness of the soil surface and litter layer above. Photosynthesis is almost entirely governed by plant responses to light, temperature, wind, and humidity, and can vary across short spatial and temporal scales depending on cloud cover and microclimate. Soil CO_2 efflux is governed by the production of CO_2, which can vary depending on soil temperature and moisture, and its conductance to the surface, which can depend on air pressure and wind speed at the soil surface and also the moisture, texture, and conduits within the soil itself. Our data suggest that Fc and LE were inherently more variable spatially than *H*, which resulted in greater variation of fluxes measured only several meters apart. Whether the soil components or plant components of Fc and LE are more spatially variable is undetermined by this study.

Cooper et al. (1992) used an array of five EC and two MBR systems to measure evaporation over a level agricultural field, and found that the LE in a single time period varied by 20% across 50 m distances and up to 35% over 100 m distances. The observed variation among instruments was corroborated by comparable variability of water vapor measured by Lidar over the same domain, suggesting that the variation was due to spatial variability in the underlying ecosystem gas exchange rather than instrumental error.

The relative scatter of *H*, LE, and Fc observed in the EC-EC comparison was also observed in the measurements between EC and MBR, which showed the greatest discrepancy in Fc and greatest similarity in *H* and LE. After clear outliers are discarded, the regression slopes for *H* and LE are nearly 1, but only ~0.9 for Fc (i.e., MBR less negative than Fc). This apparently was the result of occasionally large negative fluxes in MBR, which appeared to be unusually large departures from the overall light–response curve (Fig. 4).

A key assumption in the MBR technique is that the vertical mixing coefficients (*K* in Eq. (3)) for T, CO_2, and H_2O are identical. The analysis of Barr et al. (1994) concluded that the MBR mixing coefficients were unequal during neutral conditions due to uncorrelated T and H_2O. Our study directly tested this hypothesis by comparing the discrepancy in fluxes to the correlation between CO_2, H_2O, and T (Fig. 4). We found that relative differences in the fluxes were largest during neutral conditions, when there was also large variation in the correlation coefficient between scalars, showing both high and low correlation. Neutral stability occurs when wind shear, rather than buoyancy, drives vertical mixing, and can be seen as a condition in which vertical mixing is driven by exogenous forcing rather than buoyancy originating from surface heating. The dissociation of H_2O, CO_2 and T co-transport introduces the possibility that the vertical mixing coefficient K calculated from the vertical T gradient in MBR (Eq. (3)) may not apply for CO_2 or H_2O. Because CO_2 fluxes are directly calculated on the basis of this K, periods with low correlation between T and CO_2 should be approached with caution. We have shown that these conditions occur most often when z/L approaches zero, when wind shear is high.

5. Conclusion

Eddy covariance and modified Bowen ratio systems have been shown to yield subtly different estimates of *H*, LE, and Fc. Our study analyzed the discrepancies between these two systems by first considering the role of the data processing algorithm used to estimate fluxes using EC and later examining the effects of atmospheric stability on discrepancies between EC and MBR. We found that EC correction algorithms disproportionately increase the magnitude of LE and Fc, and consequently have a strong effect on the Bowen ratio measured by EC. Two corrections not universally employed were each found to account for up to 24% of LE and Fc: the correction for signal asynchrony by adjusting the lag between the IRGA and the sonic anemometer, and the frequency domain correction for path-length averaging in both instruments. Comparison of fluxes between two EC systems 10 m apart showed that LE and Fc are inherently more variable than *H*, highlighting the role of field heterogeneity in determining canopy gas exchange at very small spatial scales.

When all relevant corrections were applied, there was no bias for *H* and LE between EC and MBR, but Fc in EC remained slightly smaller than MBR. This lack of bias indicates that the two systems could be interchangeable for the purposes of calculating long-term integrals, or fitting a model against a large ensemble of flux data. An examination of discrepancies between EC and MBR showed that the relative discrepancies were highest during neutral periods when shear drove vertical mixing much more than buoyancy. During these neutral periods, the correlation between T, H_2O, and CO_2 was much lower on average, which violates the similarity assumption exploited in the MBR technique. While *H* and LE fluxes tended to be small during these neutral periods, Fc fluxes were not. Therefore, we believe that Fc measured by MBR under neutral conditions is most likely to be compromised by failure of the assumption of similarity of vertical mixing coefficients.

The largest discrepancies in Fc in both systems were clearly visible when plotted against a light–response curve, which creates the possibility of using a screening technique to exclude data that depart markedly from other recently collected data. The EC system tended to have the largest departures from the curve when light was near zero and respiration dominated over photosynthesis. The departures from the expected value are both high and low, showing a susceptibility to transitions from stable to unstable conditions. By contrast, the MBR system tended to show much less variability at night but occasionally estimated spikes of unusually large photosynthetic uptake, which were visible both as departures from the light–response curve and from the EC and MBR time series.

Acknowledgements

This publication was made possible through support provided by US Universities, host country institutions and the Office of Agriculture and Food Security, Global Bureau, US Agency for International Development, under Grant No. PCE-G-98-00036-00. The opinions expressed herein are those of the author(s) and do not necessarily reflect the views of USAID.

REFERENCES

Angell, R.F., Svejcar, T., Bates, J., Saliendra, N.Z., Johnson, D.A., 2001. Bowen ratio and closed chamber carbon dioxide flux measurements over sagebrush steppe vegetation. Agric. Forest Meteorol. 108 (2), 153–161.

Aubinet, M., Grelle, A., Ibrom, A., Rannik, U., Moncrieff, J., Foken, T., Kowalski, A.S., Martin, P.H., Berbigier, P., Bernhofer, C., Clement, R., Elbers, J., Granier, A., Grunwald, T., Morgenstern, K., Pilegaard, K., Rebmann, C., Snijders, W., Valentini, R., Vesala, T., 2000. Estimates of the annual net carbon and water exchange of forests: the EUROFLUX methodology. Adv. Ecol. Res. 30 (30), 113–175.

Baldocchi, D., Falge, E., Gu, L., Olson, R., Hollinger, D., Running, S., Anthoni, P., Bernhofer, C., Davis, K., Evans, R., Fuentes, J., Goldstein, A., Katul, G., Law, B., Lee, X., Malhi, Y., Meyers, T., Munger, W., Oechel, W., Paw U, K.T., Pilegaard, K., Schmid, H.P., Valentini, R., Verma, S., Vesala, T., Wilson, K., Wofsy, S., 2001. FLUXNET: a new tool to study the temporal and spatial variability of ecosystem-scale carbon dioxide, water vapor, and energy flux densities. Bull. Am. Meteorol. Soc. 82 (11), 2415–2434.

Barr, A.G., King, K.M., Gillespie, T.J., Den Hartog, G., Neumann, H.H., 1994. A comparison on Bowen ratio and eddy correlation sensible and latent heat flux measurements above a deciduous forest. Boundary-Layer Meteorol. 71, 21–41.

Brotzge, J.A., Crawford, K.C., 2003. Examination of the surface energy budget: a comparison of eddy correlation and Bowen ratio measurement systems. J. Hydrometeorol. 4 (2), 160–178.

Cava, D., Contini, D., Donateo, A., Martano, P., 2007. Analysis of short-term closure of the surface energy balance above short vegetation. Agric. Forest Meteorol. 148, 82–93.

Cooper, D.I., Eichinger, W.E., Holtkamp, D.B., Karl Jr., R.R., Quick, C.R., Dugas, W., Hipps, L., 1992. Spatial variability of water vapor turbulent transfer within the boundary layer. Boundary-Layer Meteorol. 61, 389–405.

Dugas, W.A., Heuer, M.L., Mayeux, H.S., 1999. Carbon dioxide fluxes over bermudagrass, native prairie, and sorghum. Agric. Forest Meteorol. 93 (2), 121–139.

Eugster, W., Mcfadden, J.P., Chapin, E.S., 1997. A comparative approach to regional variation in surface fluxes using mobile eddy correlation towers. Boundary Layer Meteorol. 85 (2), 293–307.

Finnigan, J.J., Clement, R., Malhi, Y., Leuning, R., Cleugh, H.A., 2003. A re-evaluation of long-term flux measurement techniques. Part 1: averaging and coordinate rotation. Boundary Layer Meteorol. 107, 1–48.

Fisher, A.J., 2007. Interactive Digital Filter Design. University of York, Department of Computer Science, York, UK. http://www-users.cs.york.ac.uk/~fisher/mkfilter (accessed March 2007).

Foken, T., Wimmer, F., Mauder, M., Thomas, C., Liebethal, C., 2006. Some aspects of the energy balance closure problem. Atmos. Chem. Phys. 6, 4395–4402.

Gao, W., Coulter, R.L., Lesht, B.M., Qiu, J., Wesely, M.L., 1998. Estimating clear-sky regional surface fluxes in the southern great plains atmospheric radiation measurement site with ground measurements and satellite observations. J. Appl. Meteorol. 37 (1), 5–22.

Hall, B.D., Claiborn, C.S., 1997. Measurements of the dry deposition of peroxides to a Canadian boreal forest. J. Geophys. Res.-Atmos. 102 (D24), 29343–29353.

Hollinger, D.Y., Richardson, A.D., 2005. Uncertainty in eddy covariance measurements and its application to physiological models. Tree Physiol. 25 (7), 873–885.

Hope, A.S., Evans, S.M., 1992. Estimating reference evaporation in the central valley of California using the Linacre Model. Water Res. Bull. 28 (4), 695–702.

Lee, X.H., Finnigan, J., U, K.T.P., 2004. Coordinate systems and flux bias error. In: Lee, X.H., Massman, W.J., Law, B. (Eds.), Handbook of Micrometeorology. Kluwer, Dordrech.

Lindberg, S.E., Kim, K.H., Meyers, T.P., Owens, J.G., 1995. Micrometeorological gradient approach for quantifying air-surface exchange of mercury-vapor—tests over contaminated soils. Environ. Sci. Technol. 29 (1), 126–135.

Liu, H.P., Foken, T., 2001. A modified Bowen ratio method to determine sensible and latent heat fluxes. Meteorologische Zeitschrift 10 (1), 71–80.

Loescher, H.W., Law, B.E., Mahrt, L., Hollinger, D.Y., Campbell, J., Wofsy, S.C., 2006. Uncertainties in, and interpretation of, carbon flux estimates using the eddy covariance technique. J. Geophys. Res.-Atmos. 111 (D21).

Massman, W.J., 2000. A simple method for estimating frequency response corrections for eddy covariance systems. Agric. Forest Meteorol. 104 (3), 185–198.

Massman, W.J., Lee, X., 2002. Eddy covariance flux corrections and uncertainties in long-term studies of carbon and energy exchanges. Agric. Forest Meteorol. 113 (1–4), 121–144.

Meyers, T.P., Hall, M.E., Lindberg, S.E., Kim, K., 1996. Use of the modified Bowen-ratio technique to measure fluxes of trace gases. Atmos. Environ. 30 (19), 3321–3329.

Moncrieff, J.B., Malhi, Y., Leuning, R., 1996. The propagation of errors in long-term measurements of land-atmosphere fluxes of carbon and water. Global Change Biol. 2 (3), 231–240.

Moncrieff, J., Clement, R., Finnigan, J., Meyers, T., 2004. Averaging, detrending, and filtering of eddy covariance time series. In: Lee, X., Massman, W.J., Law, B. (Eds.), Handbook of Micrometeorology: A Guide for Surface Flux Measurement and Analysis. Kluwer, Dordrecht.

Moore, C.J., 1986. Frequency-response corrections for eddy-correlation systems. Boundary-Layer Meteorol. 37 (1–2), 17–35.

Muller, H., Kramm, G., Meixner, F., Dollard, G.J., Fowler, D., Possanzini, M., 1993. Determination of Hno3 dry deposition by modified Bowen-ratio and aerodynamic profile techniques. Tellus Series B-Chem. Phys. Meteorol. 45 (4), 346–367.

Papale, D., Reichstein, M., Aubinet, M., Canfora, E., Bernhofer, C., Kutsch, W., Longdoz, B., Rambal, S., Valentini, R., Vesala, T., Yakir, D., 2006. Towards a standardized processing of Net Ecosystem Exchange measured with eddy covariance technique: algorithms and uncertainty estimation. Biogeosciences 3 (4), 571–583.

Rissmann, J., Tetzlaff, G., 1994. Application of a spectral correction method for measurements of covariances with fast-response sensors in the atmospheric boundary-layer up to a height of 130 M and testing of the corrections. Boundary-Layer Meteorol. 70 (3), 293–305.

Schween, J.H., Dlugi, R., Hewitt, C.N., Foster, P., 1997. Determination and accuracy of VOC-fluxes above the pine/oak forest at Castelporziano. Atmos. Environ. 31, 199–215.

Twine, T.E., Kustas, W.P., Norman, J.M., Cook, D.R., Houser, P.R., Meyers, T.P., Prueger, J.H., Starks, P.J., Wesely, M.L., 2000. Correcting eddy-covariance flux underestimates over a grassland. Agric. Forest Meteorol. 103 (3), 279–300.

Webb, E.K., Pearman, G.I., Leuning, R., 1980. Correction of flux measurements for density effects due to heat and water-vapor transfer. Quart. J. Royal Meteorol. Soc. 106 (447), 85–100.

Wolf, A., Laca, E.A. Cospectral analysis of high frequency signal loss in eddy covariance measurements. Atmos. Chem. Phys., in press.

Wolf, A., Akshalov, K., Saliendra, N., Johnson, D.A., Laca, E.A., 2006. Inverse estimation of Vc(max), leaf area index, and the Ball-Berry parameter from carbon and energy fluxes. J. Geophys. Res.-Atmos. 111 (D8), S08.